Turkish Journal of Earth Sciences (Turkish J. Earth Sci.), **Vol. 15**, 2006, pp. 211-223. *Copyright ©TÜBİTAK*

Calcretized Ferricretes Around the Jaisalmer Area, Thar Desert, India: Their Chemistry, Mineralogy, Micromorphology and Genesis

DESIKAN RAMAKRISHNAN[1] & KRISHNA CHANDRA TIWARI[2]

[1]Regional Remote Sensing Service Centre (R.R.S.S.C),
Indian Space Research Organization (I.S.R.O), I.I.T Campus, Kharagpur – 721 302, India
(E-mail: aarkay_geol@yahoo.com)
[2]Department of Geology, Faculty of Science, M.S.University of Baroda, Vadodara 390 002, India

Abstract: Ferricrete, an iron duricrust, caps Tertiary and Mesozoic rocks around Jaisalmer in the Indian desert. These ferricretes are associated with two distinct present-day landforms. The upper unit is a high-level dissected, rocky structural plain and the lower one a colluvial flat with soft ferricrete gravels. This study pertains to the first situation wherein field observations, micromorphological features and regolith chemistry suggest an *in situ* origin for the ferricretes, as in the case of the Walther profile. Subsequent tectonism and changes in base level resulted in a shift in processes from weathering to erosion. Episodes of erosion resulted in inversion of relief whereby low but resistant areas with *in situ* weathering profiles remain as high-level structural plains, mesas and buttes after erosion of the softer material around them. Destruction of nodules and pisoliths, removal of nodules, and formation of cavities suggest destruction of duricrust and the associated weathering profile. A subsequent shift in climatic regime from warm humid conditions of the Neogene period to hot arid conditions of the present resulted in a change in the weathering processes from ferricretization to calcretization. In all, three phases of calcretization are superimposed on the dissected ferricrete profiles.

Key Words: ferricrete, calcrete, micromorphology, inversion of relief, Thar Desert

Jaisalmer Bölgesi Kalsitleşmiş Ferikretleri, Thar Çölü, Hindistan: Kimyası, Mineralojisi, Micromorfolojisi ve Oluşumu

Özet: Ferrikirit, demir 'duricrustı', Hindistan çölündeki Jaisalmer civarında Tersiyer ve Mesozoyik yaşlı kayaçları üzerler. Ferrikiritler iki farklı güncel yüzey şekliyle birlikte gelişmişlerdir. En üstteki birim parçalanmış kayalık yapısal bir düzlük iken allttaki ferrikrit çakıllarından oluşan yumuşak bir kolluviyal düzeydir. Bu çalışma, arazi gözlemleri, mikromorfolojik özellikler ve toprak kimyasına bağlı olarak ferrikritlerin Walther profilinde olduğu gibi yerinde oluştuğunu rapor etmektedir. Takip eden dönemde gelişen tektonizma ve temel seviyedeki değişimler etkin olan bozuşma sürecini erozyona doğru değiştirmiştir. Erozyon safhaları röliyefde terslenmelere neden olmuş; öyleki etraflarındaki yumuşak materyallerin aşınıp taşınması sonucu daha alçak kesimlerdeki dayanımlı alanlar yüksek yapısal düzlükler, mesa ve '*butle*' şeklinde korunmuşlardır. Nodüller ve pisolitlerin parçalanması, nodüllerin taşınıp-ortadan kaldırılması ve oyuk-boşlukların oluşması 'duricrust'lar ile beraberindeki günlenme profillerinin parçalanmasını öne sürmektedir. Sonrasında gelişen iklim değişiklikleri – Neojen dönemindeki sıcak ve nemli koşullardan günümüzdeki sıcak fakat kuru koşullara doğru değişim – günlenme mekanizmalarında ferrikritleşmenden kalkeritleşme doğru bir değişime neden olmuştur. Sonuçta, üç kakeritleşme fazı parçalanmış ferrikrit profillerinin üzerine gelişmiştir.

Anahtar Sözcükler: ferrikirit, kalkerit, mikromofoloji, röliyef terslenmesi, Thar Çölü

Introduction

Ever since Buchanan (1807) introduced the term "laterite", multi-disciplinary studies of iron-rich crusts have resulted in the generation of a voluminous literature pertaining to its genesis (McFarlane 1983a, b; Valeton 1983; Nahon 1977, 1986) and to its applications in geotechnical, palaeoclimatic and economic-geological research (Giddigasu 1987; Das *et al.* 1999; Ramakrishnan & Tiwari 1999).

In spite of the wealth of information now available on laterites, controversies still persist on the mode of origin of a wide variety of iron encrustations, leading to various nomenclatures – such as iron hat, ferricrete, fersilitic, fersialitic and ferralitic soils – for different types of iron

accumulation in the regolith (Nahon 1986; Aleva 1991; Bourman 1991).

In the Thar Desert of India around Jaisalmer, iron accumulations have resulted in the formation of an iron cap over sedimentary rocks. These duricrust caps are associated with high-level rocky structural plains, plateaus, mesas and buttes.

Geology

The rocks of the study area (Figure 1) consist of sedimentary sequences representing the Palaeozoic (boulder bed, sandstones and limestone), Mesozoic (sandstone, shale, limestone), Cenozoic (sandstone) and Quaternary (gravel bed, evaporates). These sedimentary rocks are – to a great extent – covered by wind-blown sands from the Quaternary period (Pareek 1981). The generalised stratigraphic sequence is given in Table 1.

Geomorphology and Morphostratigraphy

The landform features of the Jaisalmer basin (Figure 2) are heterogenous and complex. This is mainly due to the shift in climate from warm-humid (Neogene) to the present-day hot arid conditions with periodic wet (Early Pleistocene, Early Holocene) and semi-arid (Middle–Late Pleistocene) phases (Swain *et al.* 1983; Ramakrishnan 1997). Thus, Quaternary sediments of the study area are reflected in varied forms, such as residual, fluvial, lacustrine and aeolian. In the study area, most of the Tertiary and pre-Tertiary sandstones, shale and limestone, with their horizontal or gently dipping beds, have been sculpted into to high-level rocky structural plains. This geomorphic unit (with which the ferricrete is associated) has a usual landform sequence – from the escarpment towards the dip slope of a cuesta, followed by a narrow serir plain, and then a broadly convex hammada.

Dissection of this landform has in many areas resulted in the development of mesas and buttes. The low-angle pediments, with a veneer of pebbles, cover extensive areas and are generally associated with structural plains and gravelly pavements.

In this area, recession of the Tertiary sea was followed by a first phase of planation under warm humid conditions. Development of the iron duricrust is attributed to this period (Dassarma 1983). The Late Neogene–Early Quaternary period was dominated by tectonic activity, fluvial erosion and deposition. This is evidenced by fluviatile, non-fossiliferous, ferrugenised sequences of the Shumar Formation. Older flood plains and palaeochannels represent the Late Pliestocene–Early Holocene period. This was followed by another planation under aeolian conditions. During the sub-Recent to Recent periods, this area witnessed several phases of dune building and stabilization

Regolith Characteristics

In the Jaisalmer basin, ferricrete is confined to a narrow strip (Figure 3) as a capping over weathering profiles developed on sandstones (Khuiyala Formation, Sanu Formation, Lathi Formation). In general, these ferricrete profiles consist of an upper, strongly indurated, dissected iron and/or alumina-rich layer (duricrust) and a poorly preserved saprolite horizon having a gradational contact with the parent rock. In some areas the weathering profiles are completely dismantled (dissected) and blocks of oxidized ferricrete are strewn immediately atop the parent rocks. The dominant feature of the ferricrete profiles in this area is the destruction of the ferricrete capping and subsequent phases of calcrete formation.

A typical ferricrete profile (2.5–6.5 m thick) of the study area has the following sequence (Figure 4) from top to bottom: (i) ferricrete and calcretized ferricrete, (ii) mottled horizon (r_m), (iii) pallid zone (r_p), and (iv) parent rock.

Duricrust forms the uppermost horizon and is deep red in hue with a thickness varying from 0.8–4.0 m. The iron crust occurs as sheets, nodules and packed pisoliths with varying degrees of fragmentation and oxidation. The fragmented ferricrete in many places is characterised by varying degrees of calcretization, from simple fracture filling to well-developed calcretes enveloping ferricrete nodules and pisoliths. Saprolite includes both the mottled (r_m) and pallid horizons (r_p). The mottled horizon is 0.5–2 m thick with reddish-brown mottling and widely spaced pisoliths in a clayey matrix. The pallid horizon (1.0–1.5 m thick) is white to pinkish with relict sandstone fragments in a clay groundmass. The saprolite has gradational contacts with the overlying ferricrete and underlying sandstone. The parent rock is typically ferruginous sandstone belonging to the Tertiary and Jurassic periods.

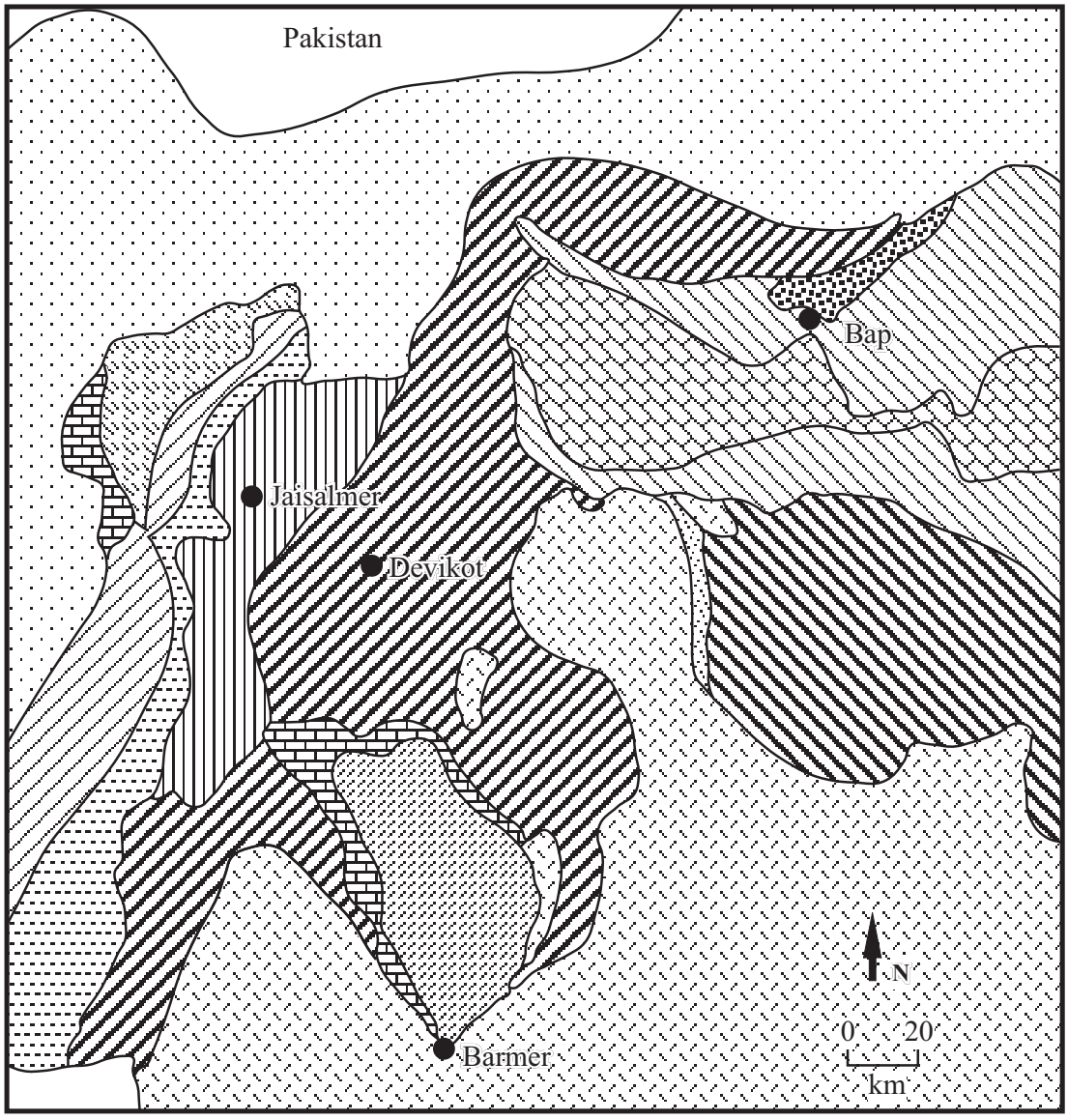

Figure 1. Regional geology of the Jaisalmer area.

Table 1. Generalised stratigraphic sequence of the study area.

Quaternary	Recent	wind-blown sand younger alluvium
	sub-recent	older alluvium Shumar gritstone
Cenozoic	Eocene	Bandah limestone Khuyala sandstone
	Palaeocene	Sanu sandstone
	major unconformity	
	Cretaceous	Abur limestone Pariwar sandstone
	unconformity	
Mesozoic	Jurassic	Bedesar sandstone Baisakhi shales Jaisalmer limestone
	unconformity	
	Lathi sandstone	
	major unconformity	
	Permo–Carboniferous	Bap boulder bed Bhadura sandstone
	unconformity	
Palaeozoic	Cambrian	Birmania limestone Randha sandstone Jodhpur sandstone Pokran boulder beds
	Major unconformity	
	Precambrian	Malani rhyolites & granites

Regolith – Landform Relationship

The landform features of the study area are mostly attributable to the pre-Neogene period, with modifications during the Neogene and Quaternary periods. Prior to these modifications, most of the study area was capped by a deeply weathered crust. Changes in the local base level due to tectonic activity resulted in the erosion of the weathered mantle in areas of high-erosion potential. Areas of low-erosion potential, such as lower slopes and valley floors, retained the original weathering profile under a blanket of transported sediments. *In situ* regolith, with a blanket of transported material occupying the tops of present day structural plain, mesas and buttes, can be attributed to inversion of relief. The fluviatile Shumar Formation, consisting of ferrugenised gravels without any continuity to the bedrock, may represent the transported ferricrete. However, this study concentrates on those ferricretes where the *in situ* weathering profile is observed in the field.

Mineralogy and Chemistry

X-ray diffraction studies (Philips PW 2070, Cu K –) of the duricrust indicate the predominance of goethite, hematite, maghemite, and quartz (Table 2). The pallid

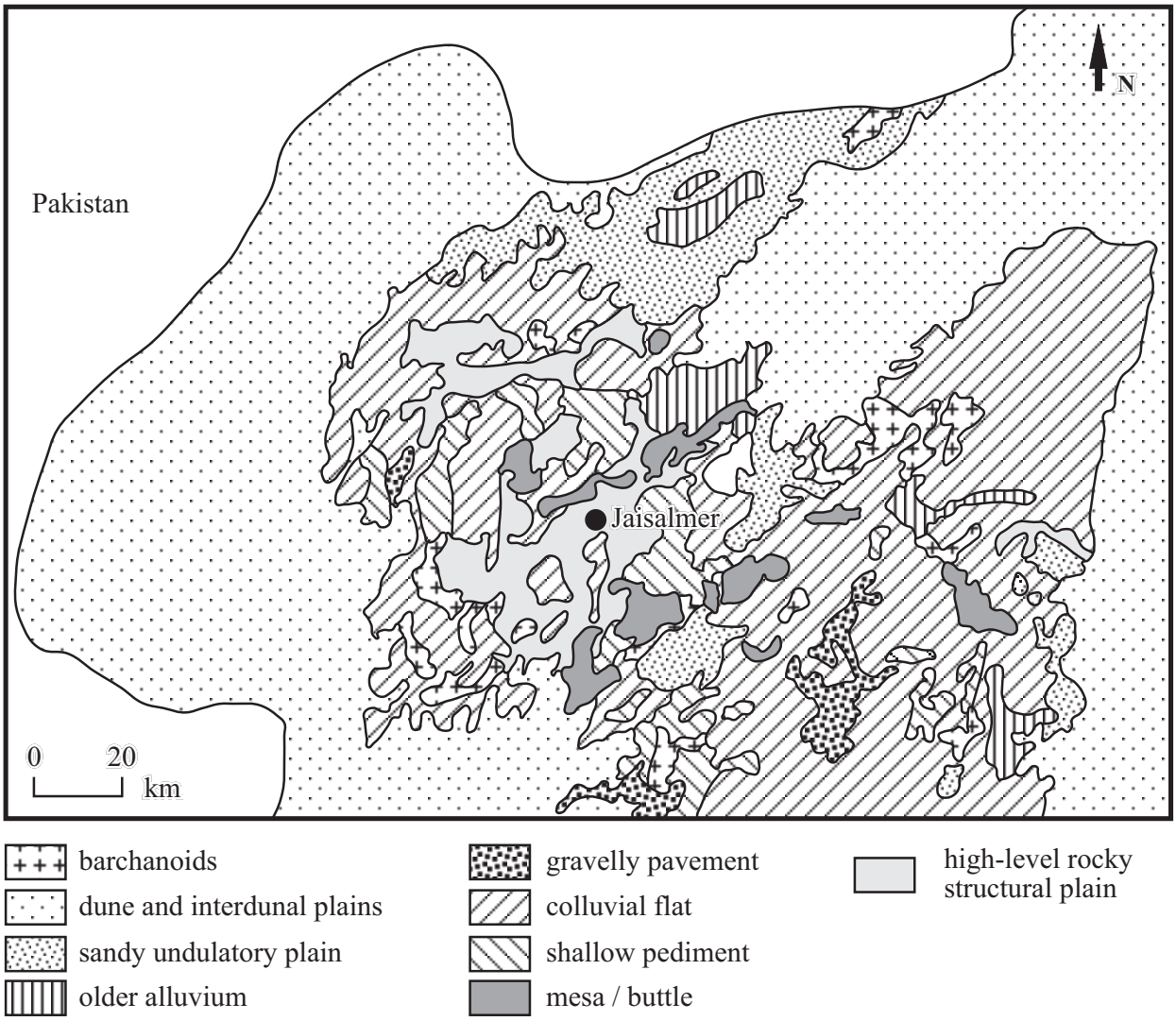

Figure 2. Geomorphological framework of the Jaisalmer area.

and mottled horizons (saprolite) consist of goethite, kaolin, montmorillonite and quartz.

Solutions of samples representing the regolith and ferricrete were prepared by the standard HF-$HClO_4$ digestion technique. An atomic absorption spectrometer (GBC-902, Australia), calibrated with USGS standards Sco-1, SGR-1 and Sdo-1, was used to estimate the chemistry. It is apparent from the results (Table 3, Figure 5) that the ferricrete is dominated by aluminium (Al_2O_3 = 16.6–24.4%) rather than iron (FeO + Fe_2O_3 = 7.6–24.9%). The weight percentages of other major oxides are silica 29–72%, CaO 2.7–22.2%, and MgO (1.0–20.3%).

Micromorphology

Poorly preserved sequences of weathering horizons, and dismantling and contamination by multiple phases of calcretization, has restricted the efficacy of conventional techniques (Fitzpatrick & Schwertmann 1982; McFarlane 1983a, b; Balasubramaniam *et al.* 1987; Das *et al.* 1999) in understanding the weathering trends, neoformations, and equlibria of different neoformed minerals from geochemical studies. Hence, micromorphological studies of ferricrete and associated weathering profiles are required to understand the processes of ferricrete genesis and development. Thin sections of duricrust and associated weathering horizons were prepared from ten

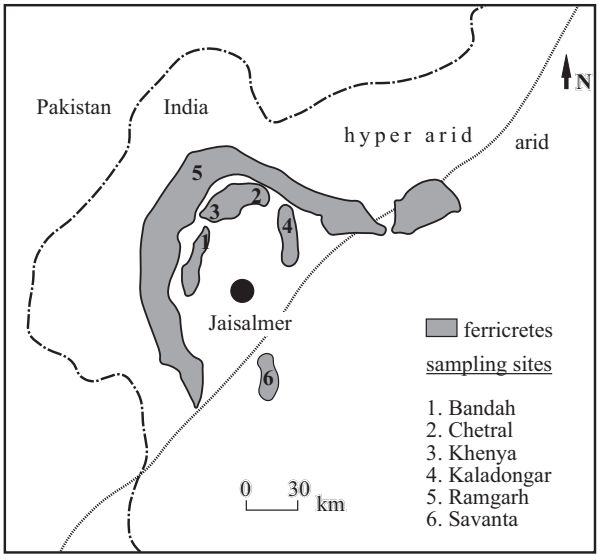

Figure 3. Distribution pattern of ferricrete in the study area.

profiles following the method of Ramakrishnan & Tiwari (1996). Some of the important micromorphological features of the representative weathering horizons are discussed here:

(i) Ferricrete (duricrust) typically shows a spongy or cellular structure (Figure 6a), locally filled with yellowish-brown iron oxides. In places, they also incorporate fibrous clayey materials. These features strongly point to *in situ* weathering in the development of duricrust (Bullock *et al.* 1985). The ferricrete consists of a few quartz detrital grains within an opaque to translucent ferruginous groundmass. These quartz grains are strongly etched, corroded and dissolved (Figure 6b), pointing to desilicification as a dominant process that operated in the upper parts of the weathering profiles.

(ii) The saprolite (r_m) horizons do not contain any relict textural features of the parent rock. Formation of iron nodules and reddish-brown mottling in a kaolin groundmass are characteristic features of this horizon. Quartz grains show etching and corrosion. The lower parts of the saprolite horizon (r_p) typically preserve the relict textural features of the parent rock (sandstone) in a clayey groundmass (Figure 6c). This feature strongly points to dominance of *in situ* weathering and neoformation of minerals.

(iii) Precipitation of secondary silica (chalcedony) within the channels and fractures is commonly observed in the mottled and pallid zones of all the investigated ferricrete profiles (Figure 6d). Precipitation of secondary silica in the lower parts of the weathering profile and the presence of etched, corroded quartz grains in the upper parts strongly indicate the role of desilicification processes in ferricrete formation. Precipitation of secondary silica also suggests changes in microenvironmental (pH) conditions in the lower parts of the weathering profile.

(iv) Destruction and erosion of the weathering profile is indicated by oxidation and solution activity along different layers of the profile. This has resulted in the formation of alternating opaque and yellowish-brown iron-oxide layers (Figure 6e). The progression of erosion has resulted in the peeling of individual layers and destruction of the weathering profile.

(v) The first phase of calcrete formation is evidenced by clear, very coarse sparitic crystals filling the vesicles, cavities and fractures (Figure 6f), and as pendant cements (Figure 6g). Micrites and sparites occur as fine laminations along the channel walls within the dismantled ferricrete.

(vi) The second phase of calcrete formation is evidenced by the presence of a drusy micritic groundmass enveloping the ferricrete nodules and calcrete fragments which developed during the first phase (Figure 6h). Advancement of calcrete formation by way of calcite neoformation has resulted in the formation of a calcrete layer. This layer of calcrete envelops relicts of ferricrete nodules and breccias. Further calcrete development has resulted in the digestion of ferricrete nodules and breccias by way of calcite replacement (Figure 6i).

Discussion and Conclusions

The ferricrete is predominantly composed of mineral assemblages such as goethite, hematite, maghemite and quartz. From the chemical analyses, it is evident that the sesquioxides are richer in alumina than in iron. This suggests that the goethite in the ferricrete is

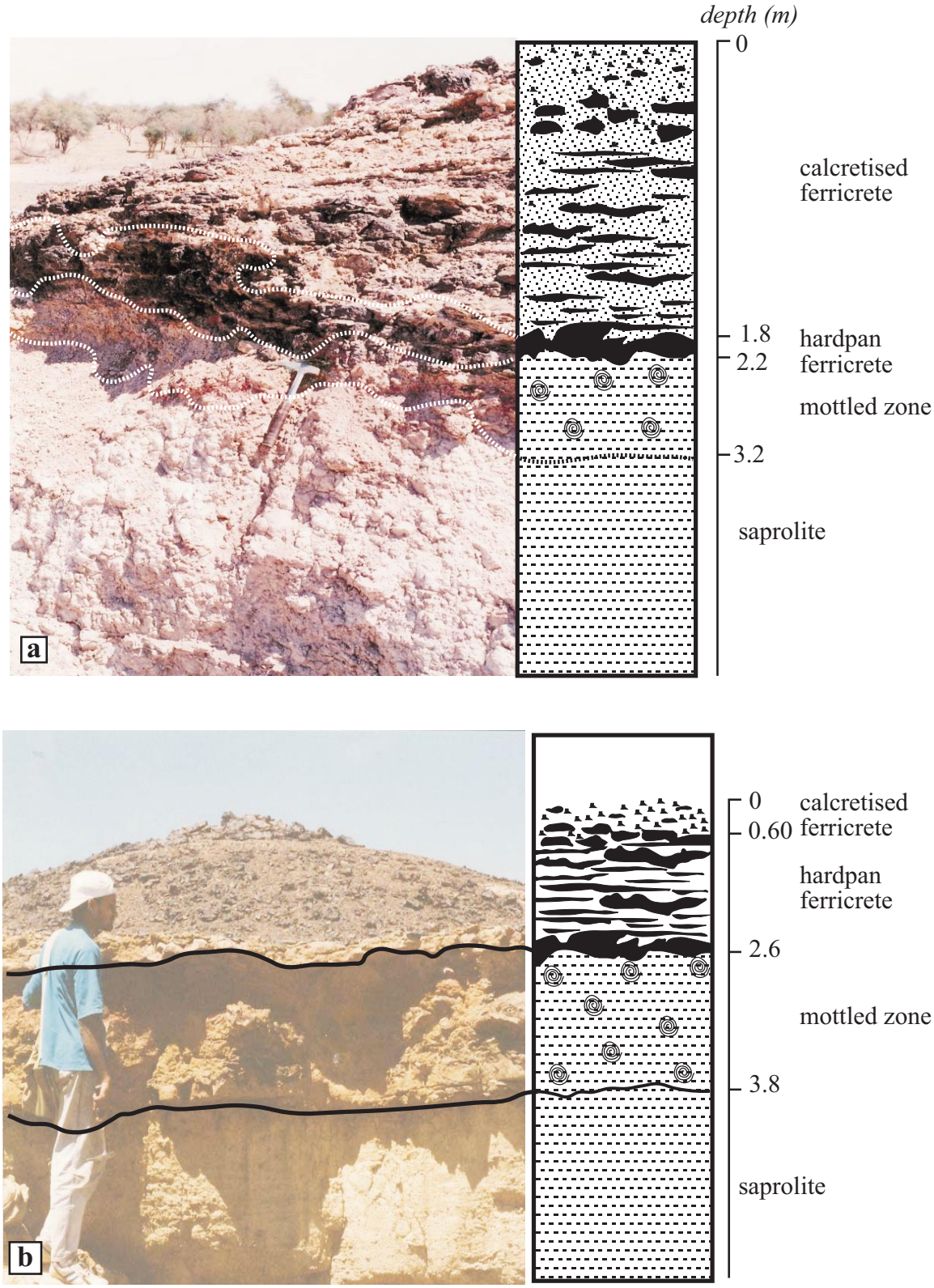

Figure 4. Field photographs showing typical calcretized ferricretes from Savanta (a) and Chetral (b) locations.

Table 2. XRD data on the mineral assemblages of the ferricrete profiles.

Location: Ramgarh	2θo	21.29	26.65	29.42	33.10	35.63	35.98	39.44	43.14	47.63	48.63					
	D (Å)	4.17	3.34	3.03	2.70	2.58	2.49	2.28	2.09	1.90	1.87					
Horizon: Duricrust	I/Io	20	39	100	18	17	17	23	13	13	17					
	Mineral	Goe	Qtz	Cal	Goe	Goe	Cal	Qtz	Cal	Cal	Cal					
Location: Ramgarh	2θo	20.90	21.18	21.40	26.65	30.34	34.55	36.51	36.60	39.45	40.31	41.06	42.45	50.14	50.31	54.86
	D (Å)	4.24	4.19	4.14	3.34	2.94	2.59	2.46	2.45	2.28	2.23	2.19	2.12	1.82	1.81	1.67
Horizon: Mottled	I/Io	30	10	11	100	9	9	13	19	9	11	8	15	17	9	8
zone	Mineral	Qtz	Goe	Magh	Qtz	Magh.	Goe	Qtz	Goe	Qtz	Qtz	Goe	Qtz	Qtz	Magh	Qtz
Location: Bandah	2θo	20.86	21.29	26.63	29.40	33.35	36.57	36.80	36.90	39.48	39.60	53.43				
	D (Å)	4.26	4.17	3.34	3.03	2.69	2.46	2.44	2.43	2.28	2.27	1.71				
Horizon: Duricrust	I/Io	25	25	100	16	10	10	15	13	12	10	9				
	Mineral	Qtz	Goe	Qtz	Calc	Goe	Qtz	Goe	Qtz	Calc	Qtz	Goe				
Location: Bandah	2θo	12.20	20.82	23.03	26.60	29.40	35.97	36.57	38.79	39.42	43.16	47.16	47.53	48.51	50.06	56.58
	D (Å)	7.25	4.26	3.86	3.34	3.03	2.50	2.45	2.32	2.28	2.09	1.93	1.91	1.88	1.81	1.63
Horizon: Mottled	I/Io	3	3	6	13	100	8	2	2	12	12	4	18	12	2	2
zone	Mineral	Kaol	Qtz	Calc	Qtz	Calc	Calc	Qz	Kaol	Qtz	Cal	Cal	Cal	Qtz	Qtz	Qtz
Location: Chetral	2θo	20.93	21.33	24.18	26.61	29.43	33.07	34.73	35.58	36.03	39.45	43.20	47.57	48.53	54.05	57.45
	D (Å)	4.24	4.16	3.68	3.34	3.03	2.70	2.58	2.52	2.49	2.28	2.09	1.90	1.87	1.65	1.60
Horizon: Duricrust	I/Io	21	14	15	77	100	27	15	18	19	33	21	24	21	16	17
	Mineral	Qtz	Goe	Hema	Qtz	Cal	Hema	Goe	Hema	Goe	Qtz	Cal	Goe	Cal	Hema	Goe
Location: Savanta	2θo	20.75	26.58	30.83	33.31	36.53	39.41	50.13								
	D (Å)	4.27	3.35	2.90	2.67	2.45	2.28	1.81								
Horizon: Duricrust	I/Io	25	100	11	11	11	11	24								
	Mineral	Qtz	Qtz	Magh	Goe	Qtz	Qtz	Qtz								
Location: Savanta	2θo	12.33	17.74	19.73	20.81	21.19	24.84	26.60	29.80	34.92	35.99	36.50	38.36	39.44	40.23	42.48
	D (Å)	7.17	5.00	4.45	4.27	4.19	3.58	3.34	3.00	2.57	2.49	2.46	2.35	2.28	2.24	2.13
Horizon: Mottled	I/Io	25	7	4	24	3	8	100	3	3	3	9	3	7	4	6
zone	Mineral	Kaol	Goe	Kaol	Qtz	Goe	Magh	Qtz	Magh	Goe	Goe	Qtz	Kaol	Qtz	Qtz	Qtz
Location: Khenya	2θo	21.32	23.10	26.60	29.45	36.06	36.90	39.48	43.25	47.74	48.60	57.48				
	D (Å)	4.17	3.85	3.34	3.03	2.48	2.43	2.28	2.09	1.90	1.87	1.62				
Horizon: Duricrust	I/Io	19	14	20	100	22	12	23	23	13	17	15				
	Mineral	Goe	Cal	Qtz	Cal	Cal	Goe	Cal	Cal	Cal	Cal	Goe				
Location: Khenya	2θo	22.85	26.42	29.25	30.46	30.58	35.78	36.62	36.78	39.31	43.03	46.94	47.06	47.35	48.41	57.35
	D (Å)	3.88	3.37	3.05	2.93	2.92	2.50	2.45	2.44	2.29	2.10	1.93	1.92	1.91	1.88	1.61
Horizon: Mottled	I/Io	12	19	100	19	17	19	8	9	23	18	8	9	16	19	10
zone	Mineral	Cal	Goe	Cal	Goe	Goe	Cal	Qtz	Goe	Cal	Cal	Goe	Cal	Cal	Cal	Goe

Calc– Calcite; Qzt– Quartz; Goe– Goethite; Kaol– Kaolin; Magh– Maghemite

Table 3. Major-oxide and trace-element chemistry of ferricrete profiles.

Location	Depth (m)	SiO_2*	FeO+ Fe_2O_3*	Al_2O_3*	CaO*	MgO*	Zn ppm	Cu ppm	Mn ppm	Sr ppm	Ba ppm	Bo ppm
Ramgarh	0.3	47.0	13.0	23.9	11.0	4.7	50	22	63	247	27	2784
	1.5	79.0	4.0	8.3	4.2	3.8	24	22	99	2786	239	3032
	2.5	74.8	3.6	16.8	0.5	4.2	42	32	66	3618	151	809
Bandah	0.5	66.3	7.6	22.3	2.7	1.1	35	15	17	134	11	350
	1.5	51.0	4.9	18.7	21.9	3.5	28	8	10	351	32	132
Chetral	2.5	52.1	10.8	24.4	9.5	3.2	83	17	61	1136	47	2115
	3.7	89.4	0.5	9.1	0.5	0.5	4	7	6	120	22	3276
Savanta	1.0	72.6	8.7	16.6	0.8	1.0	97	17	1458	262	143	nd
	1.8	72.9	2.8	18.9	4.4	1.0	60	20	45	832	49	931
	3.0	78.4	2.5	18.2	0.2	0.6	36	15	13	101	20	1985
Khenya	0.6	29.2	12.4	38.0	14.4	6.2	16	9	62	441	30	3067
	2.5	61.8	5.8	9.9	11.3	11.2	15	9	28	656	25	312
Kaladongar	2.0	19.2	24.9	13.4	22.2	20.3	38	7	160	82	17	nd
	5.0	10.6	11.2	16.8	29.2	32.1	29	3	123	249	25	1762
	10.	55.1	4.8	18.9	2.2	19.0	25	15	35	98	23	929

nd - not detected; * Major-oxide concentration in weight %.

predominantly Al-goethite (Schwertmann & Taylor 1977; Fitzpatrick & Schwertmann 1982). The high Al availability during goethite formation is attributed to a low pH and the presence of clay minerals, especially kaolin, in a leaching environment (Fitzpatrick & Schwertmann 1982).

The presence of Al-rich goethite is a good indicator of desilicification in acidic conditions (Schwertmann & Taylor 1977). The micromorphological observations also support this; that is, corrosion and dissolution of quartz in the upper horizons of the weathering profile. Disappearance of kaolin, corrosion and dissolution of quartz, and formation of Al-goethite and spongy texture are evidence of the development of ferricrete under lateritic weathering conditions (Little & Gilkes 1982; Meyer 1997).

The chemical classification based on the Al_2O_3-Fe_2O_3-SiO_2 ternary plot and the molar ratio of SiO_2/Fe_2O_3: SiO_2 / Al_2O_3 + Fe_2O_3 (Figure 5) indicate that this ferricrete is similar to *aluminous laterites* (Schellman 1981). However, classification based on the chemical data alone could be misleading (Bourman & Ollier 2002). Therefore,

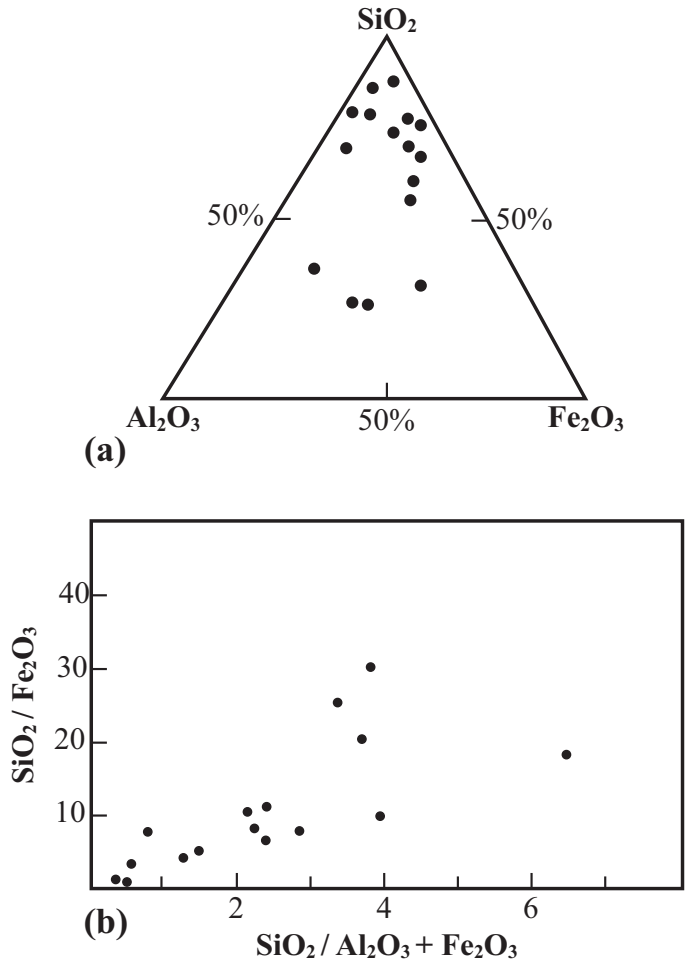

Figure 5. (a) Ternary diagram and (b) molar-ratio plots depicting the chemistry of the ferricretes.

on the basis of morphology (Bourman 1996), these ferricretes are grouped under *ferrugenised sediments* and *vermiform laterites*. The silica gel generated in the upper horizons has been precipitated as cryptocrystalline silica in the mottled horizon due to change in physicochemical conditions – from neutral to near-alkaline conditions (Balasubramaniam *et al.* 1987; Morris & Fletcher 1987; Koln 1992). The alkaline and poorly drained nature of the mottled and pallid horizons are also demonstrated by the Ba/Sr ratio (0.02–0.35) of these zones (Retallack 1990). Since the chemistry, micromorphology and field evidence strongly point to the continuity of these weathering profiles, these ferricretes can be regarded as remnants of the *Walther profile*. These weathering profiles were subsequently subjected to oxidation and solution, which ultimately resulted in breakdown of the weathering profile. The prevalence of relict micromorphological features – such as breaking of pisoliths, dissolution, and cavity generation in the dismantled weathering profiles – indicates the end of ferricrete development. This could be attributed to both changes in the base level of erosion due to tectonic activity and climatic change that the area has witnessed (Swain *et al.* 1983; Wasson *et al.* 1983). Areas of low-erosion potential, such as lower slopes, retain the original weathering profile under a blanket of transported sediments. *In situ* regolith, with a blanket of transported material occupying the tops of present-day structural plain, mesas and buttes, can be attributed to inversion of relief (Figure 7). However, palaeo-drainage channels, outlined by duricrust-capped mesas and buttes (Pain & Ollier 1995), are not present in the study area.

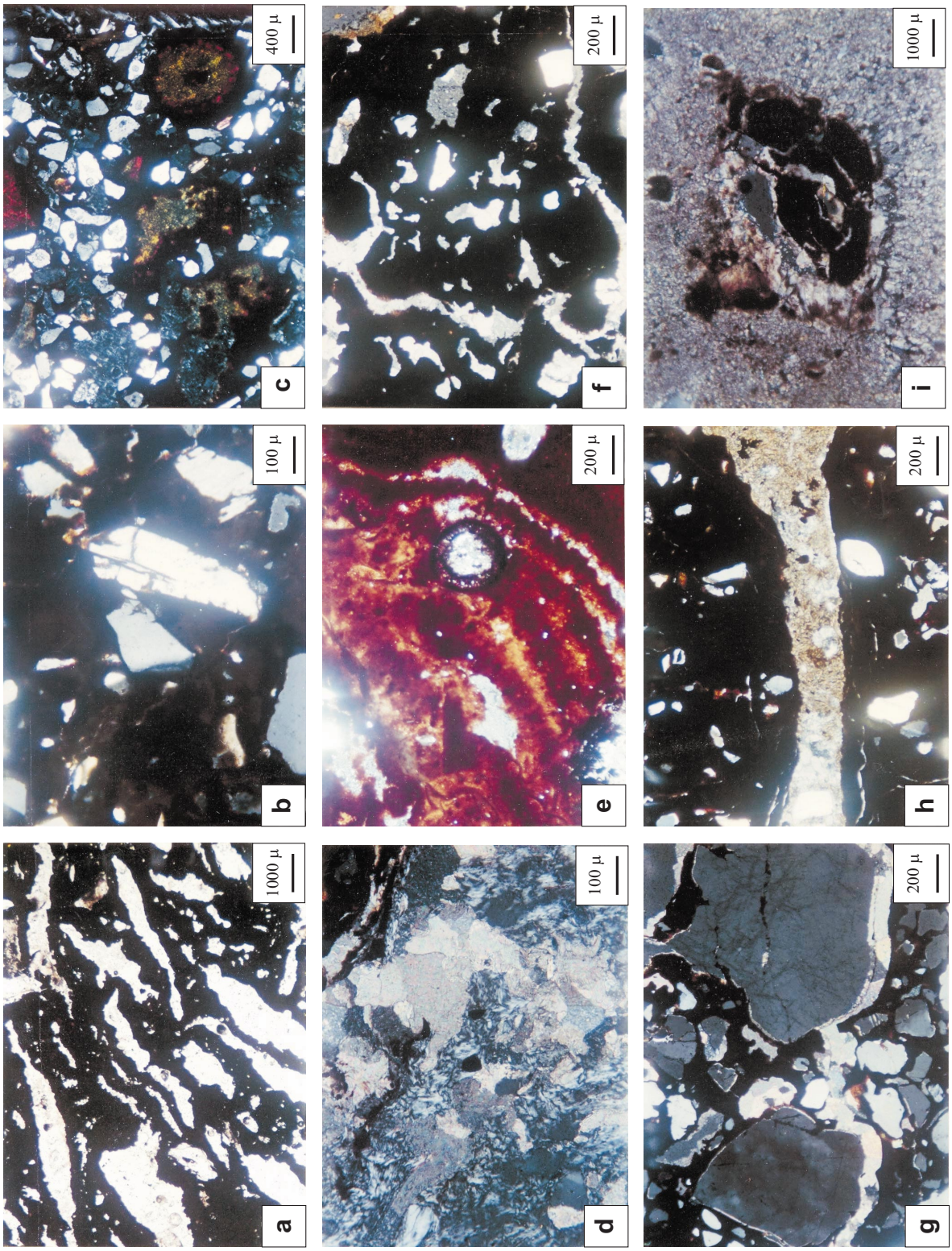

Figure 6. Micromorphological features of the ferricrete profiles: (a) vesicular structure; (b) *in situ* dissolution of quartz; (c) iron mottling; (d) precipitation of secondary silica; (e) dissolution of pisoliths; (f) sparites filling desiccation cracks; (g) pendent cements; (h) neoformed microsparites; and (i) replacement of goethite by calcite.

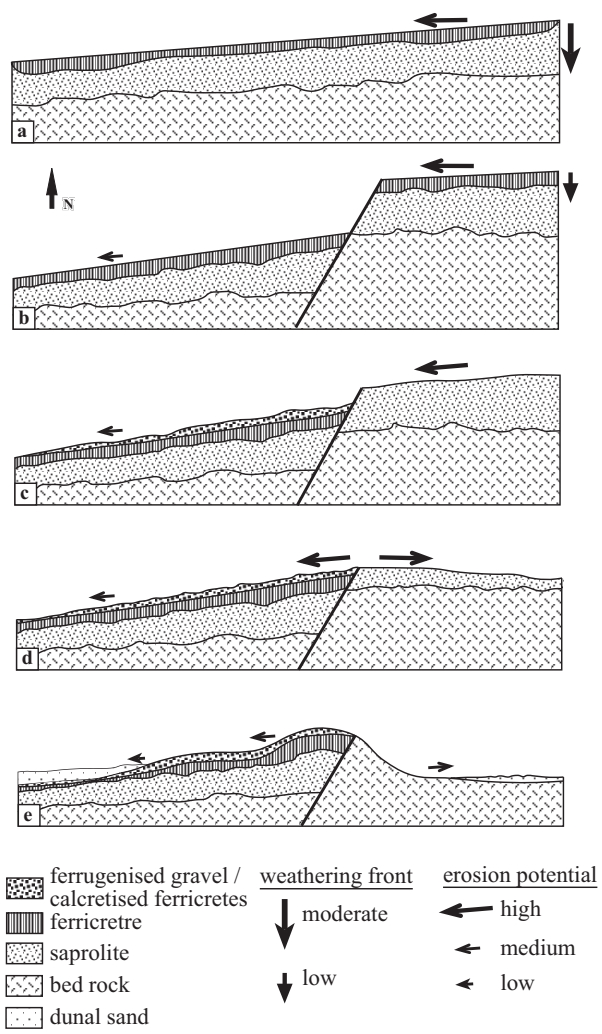

Figure 7. Schematic diagram presenting the geomorphology and regolith evolution of the Jaisalmer area.

Superimposition of calcretization on the dismantled ferricrete evidently occurred in three phases. The first phase is marked by coarse, clear sparites occurring as fracture and vesicle infillings and as pendant cements. The second phase is represented by formation of a calcrete layer, with a drusy micritic groundmass enveloping the fragmented ferricretes and first-phase calcite. The third phase is marked by the neoformation of sparites and their replacement of ferricrete fragments. These features indicate a shift in weathering processes from ferricretization to calcretization, which may have been triggered by climatic changes that the area experienced since the Neogene period (Singh & Ghose 1977; Wasson *et al.*1983; Ramakrishnan 1997).

It is evident from the foregoing account that, in the study area, ferricrete formed due to *in situ* weathering similar to the *Walther profile*. Tectonic activity and change in the base level of erosion resulted in inversion of relief, which resulted in the present-day regolith landform association. Shift in climatic conditions from warm-humid to hot-arid is responsible for change in the weathering process, thereby resulting in the destruction of ferricretes and in subsequent phases of calcretization.

Acknowledgement

The authors are grateful to referee Dr Colin F. Pain (Geoscience Australia, Canberra) for his suggestions and personal interest in this work.

References

ALEVA, G.J.J. 1991. Ferricrete. *Catena* **18**, 583–584.

BUCHANAN, F. 1807. *A Journey from Madras Through the Countries of Mysore, Canara and Malabar, 2.* East India Company, London.

BALASUBRAMANIAM, K.S., SURENDRA, M. & RAVIKUMAR, I.V. 1987. Genesis of certain bauxite profiles from India. *Chemical Geology* **60**, 227–235.

BOURMAN, R.P. 1991. *Modes of Ferricrete Genesis: Eevidence from Southeastern Australia.* Eurolat' 91, Berlin.

BOURMAN, R.P. 1996. Towards distinguishing transported and in situ ferricretes: data from southern Australia. *Australian Geological Survey Organisation (AGSO) Journal of Australian Geology and Geophysics* **16**, 231–241.

BOURMAN, R.P. & OLLIER, C.D. 2002. A critique of the Schellmann definition and classification of laterite. *Catena* **47**, 117–131.

BULLOCK, P., FEDOROFF, N., JONGERIUS, A., STOOPS, G. & TURSINA, T. 1985. *Handbook for Soil Thin-Section Description*. Wine Research Publication, England.

DAS, S.K., SAHOO, R.K., MURALIDHAR, J. & NAYAK, B.K. 1999. Mineralogy and geochemistry of profiles through lateritic nickel deposits at Kansa, Sukinda, Orissa. *Journal of the Geological Society of India* **53**, 649–668.

DASSARMA, D.C. 1983. *Climatostratigraphic Elucidation and Preparation of Quaternary Morphostratigraphic Map of Rajasthan*. Unpublished Report. Geological Survey of India, Jaipur.

FITZPATRICK, R.W. & SCHWERTMANN, U. 1982. Al-substituted goethite – an indicator of pedogenic and other weathering environments in South Africa. *Geoderma* **27**, 335–347.

GIDDIGASU, M.D., ASANTE, S.P.K. & DOUGAN, E. 1987. Identification of suitable non traditional tropical and residual paving material in relation to the environment. *Canadian Geotechnical Journal* **24**, 58–71.

KOLN, H.B. 1992. Palaeotropical weathering on different rocks in southern Germany. *Zeitschrift fuer Geomorphologie* **91**, 95–108.

LITTLE, I.P AND GILKES, R.J. (1982). Aluminum substitution in goethites in soils from alluvium, Gippsland, Victoria. *Australian Journal of Soil Research* **20**, 351–355.

MCFARLANE, M.J. 1983a. A low level laterite profile from Uganda and its relevance to the question of parent material influence on the chemical composition of laterites. *In*: WILSON, R.C.L. (ed), *Residual Deposits-Surface Related Weathering Process and Materials*. Blackwell Scientific Publishers, London, 69–76.

MCFARLANE, M.J 1983b. Laterites. *In*: GOUDIE, A.S. & PYE, K. (eds), *Chemical Sediments and Geomorphology*. Academic Press, London, 7–58.

MEYER, R 1997. *Palaeoalterites and Palaeosols – Imprints of Terrestrial Process in Sedimentary Rock.* Oxford & IBH publication, New Delhi.

MORRIS, R.C. & FLETCHER, A.B. 1987. Increased solubility of quartz following ferrous - ferric iron reactions. *Nature* **330**, 558–561.

NAHON, D.B. 1977. Time factor and geochemistry of iron crust genesis. *Catena* **4**, 249–254.

NAHON, D.B. 1986. Evolution of iron crusts. *In*: COLMAN, S.M. & DETHIER, D.P. (eds), *Rates of Chemical Weathering of Rocks and Minerals.* Academic Press, New York, 169–192.

PAIN, C.F & OLLIER, C.D. 1995. Inversion of relief – a component of landscape evolution. *Geomorphology* **12**, 151–165.

PAREEK, H.S. 1981. Basin configuration and sedimentary stratigraphy of western Rajasthan. *Journal of the Geological Society of India* **22**, 517–527.

RAMAKRISHNAN, D. 1997. *Calcretic and Ferricretic Duricrusts of the Thar Desert: Their Palaeoclimatic Significance and Geotechnical Efficacy as an Alternate Pavement Aggregate*. PhD thesis, M.S. University of Baroda, Vadodara, India [unpublished].

RAMAKRISHNAN, D. & TIWARI, K.C. 1996. Impregnation of friable sediments using solvent cement – a new standard method. *Journal of the Geological Society of India* **48**, 589–590.

RAMAKRISHNAN, D. & TIWARI, K.C. 1999. Calcretic and Ferricretic duricrusts of the Thar Desert, India: their geotechnical appraisal as a road paving aggregate. *Engineering Geology* **53**, 13–22.

RETALLACK, G.J. 1990. *Soils of the Pat - An Introduction to Palaeopedology.* Unwin Hyman Inc., New York.

SCHELLMANN, W. 1981. Consideration on the definition and classification of laterites. *Proceedings of International Semposium on Lateritization Process*. Oxford & India Book House Publication, New Delhi, 1–10.

SCHWERTMANN, U. & TAYLOR, R.M. 1977. Iron oxides. *In*: DINAUER, R.C. (ed), *Minerals in Soil Environment.* Soil Science of America Publication, Wisconsin, 145–180.

SINGH, S. & GHOSE, B. 1977. Geomorphology of the Luni basin and its palaeoclimatic inferences. *In*: AGRAWAL, D.P & PANDEY, B.M (eds), *Ecology and Archaeology of Western India.* Concept Publications, New Delhi, 135–147.

SWAIN, A.M., KUTZBACH, J.E. & HASTENRATH, S. 1983. Estimates of Holocene precipitations for Rajasthan, India based on pollen and lake level data. *Quaternary Research* **19**, 1–17.

VALETON, I. 1983. Palaeoenvironment of lateritic bauxites with vertical and lateral differentiation. *In*: WILSON, R.C.L. (ed), *Residual Deposits: Surface Related Weathering Process and Materials*. Blackwell Scientific Publication, London, 69–76.

WASSON, R.J., RAJAGURU, S.N., MISRA, V.N., AGRAWAL, D.P., DHIR, R.P. & SINGHVI, A.K. 1983. Geomorphology, Late Quaternary stratigraphy of the Thar dune field. *Zeitschrift fuer Geomorphologie* **28**, 203–220.

Received 03 November 2004; revised typescript accepted 25 November 2005